Spectroscopic factors measured in inclusive proton-knockout reactions on ^{8}B and ^{9}C at intermediate energies

J. Enders,[1,*] T. Baumann,[1] B. A. Brown,[1,2] N. H. Frank,[1,2] P. G. Hansen,[1,2,†] P. R. Heckman,[1,2] B. M. Sherrill,[1,2] A. Stolz,[1] M. Thoennessen,[1,2] J. A. Tostevin,[3] E. J. Tryggestad,[1,‡] S. Typel,[1,§] and M. S. Wallace[1,2]

[1]*National Superconducting Cyclotron Laboratory, Michigan State University, East Lansing, Michigan 48824, USA*
[2]*Department of Physics and Astronomy, Michigan State University, East Lansing, Michigan 48824, USA*
[3]*Department of Physics, School of Electronics and Physical Sciences, University of Surrey, Guildford, Surrey GU2 7XH, United Kingdom*

The knockout of protons from ^{8}B and ^{9}C on a carbon target has been studied at average energies of 76 and 78 MeV/nucleon, respectively, with beams from the A1900 fragment separator incident on a stack of silicon detectors. The following cross sections were obtained: $\sigma_{-1\mathrm{p}}(^8\mathrm{B}\rightarrow{}^7\mathrm{Be})=130(11)$ mb, $\sigma_{-1\mathrm{p}}(^9\mathrm{C}\rightarrow{}^8\mathrm{B})=54(4)$ mb, and $\sigma_{-2\mathrm{p}}(^9\mathrm{C}\rightarrow{}^7\mathrm{Be})=98(7)$ mb. The results are discussed within the framework of an eikonal approach and compared with measurements performed at higher energies. From this analysis, a consistent picture emerges that gives evidence for the validity of the eikonal approach at energies below 100 MeV/nucleon. Knockout reactions at intermediate energy can thus be used to deduce absolute shell occupancies. We find the spectroscopic factors to be reduced by R_s of 0.86(7) and 0.82(6) for ^{8}B and ^{9}C, respectively, relative to shell-model predictions. The ^{9}C result provides an accurate measurement of the asymptotic normalization coefficient of 1.27(10) fm^{-1}. A new technique is reported for determining separately the contributions from stripping and diffractive breakup.

I. INTRODUCTION

Correlations are at the heart of the nuclear shell model. Although this model starts from a picture based on noninteracting nucleonic orbitals in a central field, there are, in fact, only a few nuclei near double-closed shells that are directly amenable to such a simple approach. The correlations arising from the long-range part of the nucleon-nucleon force usually make it necessary explicitly to take into account the mixing of many valence configurations. For lighter nuclei, such as those discussed in this paper, it is possible to apply a microscopic description involving the diagonalization of a large matrix representing the (effective) interactions in a restricted quantum-mechanical space.

Hence, measuring the occupancies of single-particle orbitals in atomic nuclei is crucial for understanding the structure of a nucleus at the microscopic level. For a long time nuclear physics has investigated the states in and near stable nuclei through single-particle transfer reactions, typically analyzed by means of the distorted-wave Born approximation [1]. It is clearly difficult but not impossible to extend this technique to rare radioactive species available only in minute quantities. It has recently become clear, see, e.g., Refs. [2–7], that a powerful alternative to the removal reactions such as (p,d), (d,t), and $(d,{}^3\mathrm{He})$ is to study high-energy removal ("knockout") on light targets. Since these reactions have

multibody final states, it becomes mandatory, especially in more complex nuclei, to tag the final state populated in the knockout process by the detection of γ rays emitted by the (fast) residue. The reference (single-particle) cross sections are calculated theoretically from an eikonal approach, see Tostevin [8] and also Hencken *et al.* [9]. In this the reaction to each final state proceeds via two separate channels. The first, usually the dominant one, is referred to as stripping or inelastic breakup, a process in which the removed nucleon reacts with and excites the target. In the second, referred to as diffractive or elastic breakup, the removed nucleon is present in the forward beam with essentially beam velocity, and the target remains in its ground state. In addition, Coulomb breakup must often be taken into account. The spectroscopic factors, obtained in a series of experiments in the p and sd shells [7], indicate that knockout reactions give a consistent and accurate picture of the makeup of the many-body wave function and of the effects of long-range correlations.

A second source of correlations in the single-particle motion in a "real" nucleus is the repulsive short-range part of the nucleon-nucleon interaction, see the review by Pandharipande *et al.* [10]. Since this force sets in strongly at distances below 0.4 fm, it follows from the uncertainty principle that it must lead to components with high momentum in the nucleon wave functions. These components are hard to view directly. They are mainly conspicuous through reduced occupancies of the nucleon single-particle states in low-lying states relative to the occupancies calculated in the shell model with effective interactions, which does not incorporate these effects. It is generally believed that the quasielastic knockout from high-energy electron scattering of the type $(e,e'p)$ furnishes a superior standard for absolute spectro-

———
*Present address: Institut für Kernphysik, Technische Universität Darmstadt, Germany.
†Email address: hansen@nscl.msu.edu
‡Present address: IPN-Orsay, France.
§Present address: GSI, Darmstadt, Germany.

scopic factors, see the review by Kramer *et al.* [11]. They find occupancies in well-bound magic and near-magic nuclei that are only 0.5–0.6 relative to shell-model calculations.

It has recently been suggested [12] that knockout reactions furnish an interesting alternative method for determining spectroscopic factors on an absolute scale. Comparing the results of inclusive proton knockout reactions from ^{16}O and ^{12}C at energies at and above 250 MeV/nucleon, spectroscopic factors could be deduced that are in good agreement with the $(e,e'p)$ analyses [12]. It was pointed out that the knockout process allows one also to measure unstable isotopes as provided by today's fragmentation facilities, and makes it possible to investigate the neutron occupancies. As would be expected from isospin symmetry for these $N=Z$ nuclei, the neutron and proton occupancies agree. The analysis of Ref. [12] showed that the eikonal theory leads to consistent spectroscopic factors over a wide energy range, from 140 to 2100 MeV/nucleon. The theoretical basis for this analysis has been discussed by Tostevin [8]. However, it is unknown to which extent this holds also for the experimentally very important energy range of $E \approx 50$–100 MeV/nucleon. A theoretical analysis finds [13] that the eikonal analysis is valid down to about 20 MeV/nucleon to within $\sim 20\%$.

We present here the results of precise inclusive measurements of proton knockout from ^{8}B and ^{9}C at energies of 76.4 and 78.3 MeV/nucleon, respectively. The main aim is to extend the analysis of the spectroscopic factors [12] to lower incident beam energies. Since this analysis was based on data from carbon targets, it was decided to use a carbon target also in the present work. The knockout cross sections for the nuclei ^{8}B and ^{9}C are also important for understanding proton capture in astrophysical environments. Several recent studies give results for the nucleus ^{9}C [14–18], which will be discussed in Secs. III C and III D dealing with structure and links to nuclear astrophysics.

II. EXPERIMENT

A. Experimental technique

The experiment was carried out utilizing the A1900 fragment separator [19] at the newly commissioned Coupled-Cyclotron Facility [20] at the National Superconducting Cyclotron Laboratory (NSCL) at Michigan State University. The beams have been produced by fragmentation of a 140 MeV/nucleon ^{16}O beam. An achromatic acrylic wedge was used to select primarily the desired isotope. The stack of six silicon detectors shown in Fig. 1 was placed at the final focus of the A1900 spectrometer to identify the incoming beam as well as the breakup products. The stack consisted of three 500-μm-thick Si surface barrier detectors (labeled in the following as detectors 0–2) followed by three 5000-μm-thick Li-drifted Si diodes for total energy determination (labeled 3–5). A position-sensitive Parallel-Plate Avalanche Counter (PPAC) detector in front of the stack allowed the incoming beam angles to be restricted, and a PIN diode and a scintillator at the back of the setup were used for initial beam characterization as well as the measurement of outgoing particles. A 146-mg/cm^2-thick C target could be placed between
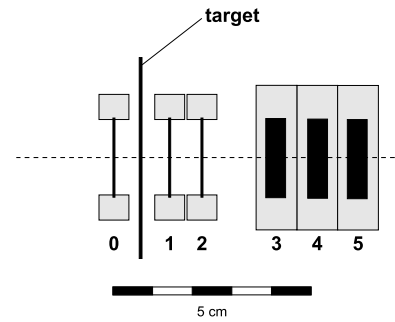

FIG. 1. The stack of silicon detectors used for identifying projectile and reaction residues. Three 500-μm-thick Si surface barrier detectors labeled detectors 0–2 are followed by three 5000-μm-thick Li-drifted Si diodes, labeled 3–5. A position-sensitive PPAC detector in front of the stack allowed the incoming beam angles to be restricted. A 146-mg/cm^2-thick C target could be placed between detectors 0 and 1.

detectors 0 and 1 of the stack. Target-out runs were performed to subtract background contributions from breakup in the detector system. Table I summarizes the details of the experiment and gives the average energies at midtarget, beam intensities, purities, and data acquisition times.

Reactions of the projectile and reaction residue in the detector stack give rise to two corrections. The main one comes from reactions taking place close to the back surface of detector 0 (i.e., before the target) and near the front surface of detector 1. These reactions have the appearance of a true event with charge Z coming in, $Z-1$ going out. This effect was measured in the target-out run and subtracted from the real events, a correction that for both projectiles was close to 25%. The projectile identification depended on the measurement of energy loss in detector 0 and the time of flight. By keeping the beam energy unchanged in the target-out run we could be sure that the background subtraction relied on graphical cuts identical to those used for the target-in runs. It is clear that this also gives the correct energy in detector 0. A simple estimate shows that the higher energy (without the target) in detector 1 does not affect the background subtraction. For the case of ^{9}C, the energy shift amounted to 4.6 MeV/nucleon; a calculation in the eikonal model shows that this decreases the 83-mb single-particle (^{9}C, ^{8}B) cross section on silicon by 0.64 mb, or by 0.8%. With an estimated one half of the 25% correction coming from detector 1, the effect would be a negligible 0.1% out of the 25%. The second, smaller, correction comes from residues lost through

TABLE I. Summary of the experiment: Average energies at midtarget, beam intensities, beam purities, and data acquisition times. Data separated by a slash (/) distinguish between runs with and without target.

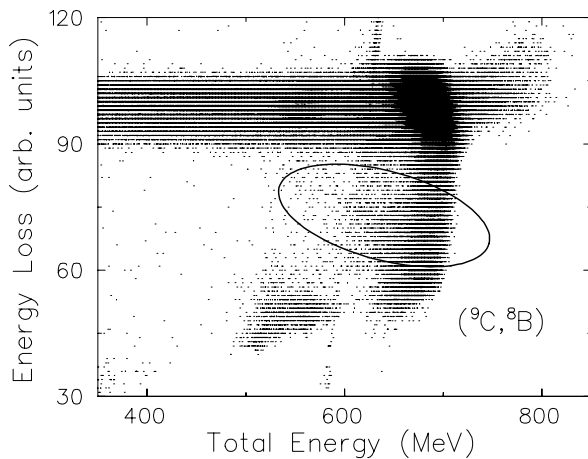|	^{8}B	^{9}C
Average energy (MeV/nucleon)	76.4	78.3
Beam intensity (s^{-1})	650/200	200/150
Beam purity (%)	83/47	82/83
Data acquisition time (h)	4.4/4.7	9.7/10.7

FIG. 2. Energy loss in detector 1 vs total energy for the example of the $(^9C, ^8B)$ reaction. The main intensity stems from the direct beam; the marked area shows the region where the residues of the one-proton knockout process reside.

reactions in detectors 1,2,3 of the stack. For the relevant energy range, 71 to 27 MeV/nucleon for ^8B, 71 to 42 MeV/nucleon for ^7Be, the average reaction cross sections (calculated) are 1.59 and 1.45 b, leading to upward corrections of the event rates of 4.8% and 4.3%, respectively. The increase in energy for the target-out run is smaller than the intrinsic spread in energy of the A1900 beam and does not affect the identification of the residues based on the integral energy loss in detectors 3 and 4 described below. (The events fall exactly on the same general curves.)

B. Data analysis

The incoming ions were identified by energy loss in detector 0 and time of flight with respect to the rf signal of the accelerator. Breakup products were selected in the following detectors. First, cuts in an energy loss versus total energy plot were made. This is indicated in Fig. 2 for the example of the $(^9C, \ ^8B)$ reaction, requiring good particle identification of ^9C in detector 0. The main intensity is the direct beam slowing down and stopping in the detector stack. The marked area shows the ^8B fragments produced in the reaction, identified by their smaller energy loss and total energy smaller by 1/9th. Such cuts were defined for the energy loss both in detector 1 and 2.

Figure 3(a) displays a plot of the energy loss in detector 3 (the first thick detector, abscissa) and the remaining energy in detector 4 (ordinate) after applying the cuts mentioned above. For the $(^9C, \ ^8B)$ reaction, the direct beam and the ^8B breakup fragments are stopped in detector 4, whereas ^7Be (not visible in Fig. 3) partially punches through detector 4 into detector 5. One recognizes part of the direct beam on the right, and a double structure at the center of the figure. The double structure stems from a difference in the energy deposition by the stripping process and the diffractive breakup. In the latter case the outgoing proton deposits additional energy, which becomes visible in the thick detectors. The lower part (b) of the figure shows the same coordinates requiring also a particle in one of the following detectors (detector 5, PIN
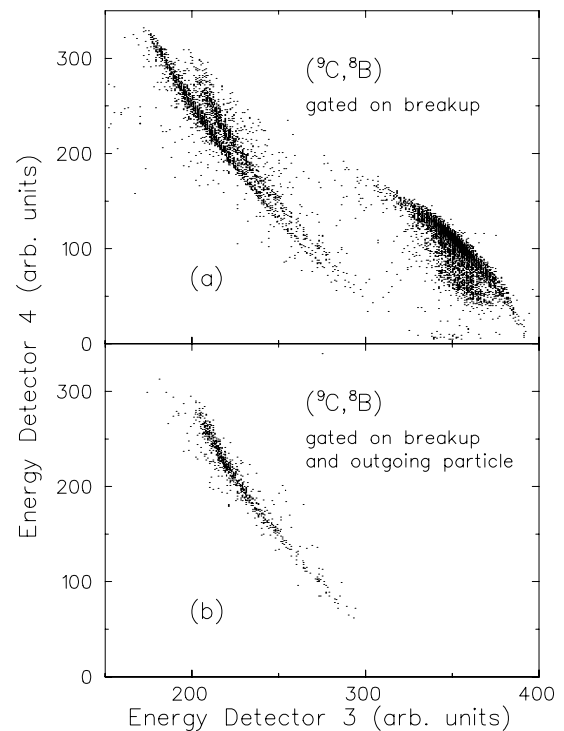

FIG. 3. Energy deposited in detectors 3 (abscissa) and 4 (ordinate) for the $(^9C, ^8B)$ reaction. Part (a) is with gates on breakup products from Fig. 2 only; in (b) the detection of an outgoing particle in detector 5, the PIN diode, or the scintillator was additionally required. The gate on the outgoing particle tags the diffractive breakup channel that can be identified as the upper branch of the double structure in part (a). The other branch is due to the stripping process. The high-intensity signal in part (a) is from the direct beam.

diode, or scintillator). Owing to the long range of the proton, this identifies the diffractive breakup channel unambiguously. The gains in the last detectors were not optimized to detect the outgoing protons, leading to a limited efficiency, and a very precise separation of the two branches visible in the figure was not possible. Various gates and cuts in the aforementioned parameters have been used to obtain an estimate on the systematic uncertainties in the analysis. This procedure was also done for the runs without target for background subtraction.

To estimate the total uncertainty in the determination of the cross section, contributions from the systematic uncertainties due to the choice of the cuts, statistical uncertainties, and an overall uncertainty of 5% for target thickness were taken into account. The contributions were added in quadrature. The analysis was done for runs with and without target.

C. Theoretical analysis

The analysis of the knockout cross sections has been discussed in several papers [5,8] and applied to the case of ^8B [12].

For clarity, some formulas are repeated here in the form appropriate for the reaction $(^9C, \ ^8B)$ with some simplifications in the notation. Because the ground state is the only

TABLE II. Summary of the experimental and theoretical results. All cross sections are in mb and the excitation energy of the final level E_f in MeV. The notation is discussed in Sec. II C. Note that the theoretical cross sections σ_{th} include a center-of-mass correction $A/(A-1)$ and for the case of ^{9}C a mismatch factor. For the experimental cross sections the separate contributions from stripping and diffraction-plus-Coulomb are shown. The quantity R_s is the short-range reduction factor discussed in the text.

Reaction	E_f	σ_{str}	σ_{diff}	σ_{C}	C^2S	σ_{th}	$\sigma_{\text{exp}}^{\text{str}}$	$\sigma_{\text{exp}}^{\text{diff}+\text{C}}$	σ_{exp}	R_s
$(^8\text{B},^7\text{Be})$	0.00	64.8	36.5	7.7	1.036	129.1				
	0.43	56.9	28.2	3.4	0.220	22.3				
	Sum					151.3	93(16)	37(13)	130(11)	0.86(7)
$(^9\text{C},^8\text{B})$	0.00	43.9	18.7	1.1	0.94	65.7	40(5)	14(4)	54(4)	0.82(6)
$(^9\text{C},^7\text{Be})$	Sum					166[a]			98(7)	

[a]See text for a detailed discussion.

bound final level, the final-state quantum numbers can be suppressed in the notation. Also, following the usual practice of adjusting the single-particle wave functions to reproduce the experimental nucleon separation energy, the $0p_{3/2}$ and $0p_{1/2}$ wave-function components will have the same radial behavior, and can be represented by a single spectroscopic factor C^2S corresponding to the sum for these two components. The theoretical cross section is then

$$\sigma_{\text{th}} = \frac{A}{A-1} C^2 S M (\sigma_{\text{str}} + \sigma_{\text{dif}} + \sigma_{\text{C}}). \quad (1)$$

Here $A/(A-1)$ is a center-of-mass correction [21] valid for the p shell, and σ_{str} and σ_{dif} are the single-particle cross sections for stripping and diffraction calculated as in the papers cited above and listed for each case in Table II. The cross sections for Coulomb dissociation σ_{C} were calculated from expressions given by Typel and Baur [22].

The quantity M, introduced in Ref. [4], is a radial mismatch factor. It takes into account the imperfect overlap of the least bound nucleon's single-particle state in the residue with its original configuration in the projectile, due to the change in the average potential between these nuclei. It is calculated as the square of the overlap integral between the radial wave functions of these single-particle states, see also Ref. [7]. It may be viewed as a small correction to our spectroscopic factors, which are obtained from a shell-model description that does not include continuum states. In essentially all cases M is unity, but the correction may become of some importance if this initial or final state nucleon orbital is close to a particle threshold.

In the case of the $(^9\text{C}, ^8\text{B})$ reaction, these proton separation energies differ by almost a factor of 10 between the initial and final states, with the final state proton bound by only 0.137 MeV. Nevertheless, the initial and final proton single-particle wave functions are very similar because of the Coulomb barrier, and the square of the radial overlap integral amounts to a small correction, $M = 0.976$. (The correction can be more important for neutrons, cf. the stripping of a neutron from ^{12}Be to the two $\ell = 0,1$ halo states of ^{11}Be [4].)

As mentioned in Sec. I, the main purpose of this paper is to search for possible deviations in the experimental cross sections that can be attributed to the effect of short-range correlations arising from the nucleon-nucleon force. To this

end, we define a reduction factor $R_s = \sigma_{\text{exp}}/\sigma_{\text{th}}$, where the theoretical spectroscopic factors entering in σ_{th} are from shell-model calculations that do not include the effects of the nucleon-nucleon hard core. In order for R_s to be more than an empirical scale correction, it is clearly essential that the structural model used as the reference is accurate. Most previous work based on the $(e,e'p)$ reaction has used closed-shell systems as the reference; we argue below that also our cases in the p shell are sufficiently well under control to furnish a scale of comparison.

Although the possible role of ^{9}C in nuclear astrophysics is out of the scope of this paper, we also discuss briefly how the result of the present work fits in with other recent results for this nucleus. The essential quantity of interest is the large-distance behavior of the bound-state wave function. It is useful for this purpose to introduce an asymptotic normalization coefficient C_ℓ^2, see Ref. [23] and earlier work cited therein. It is defined by equating the "true" radial wave function, expressed as the product of structure factors and a radial single-particle wave function $R(r)$, normalized to unity $\int R^2(r) r^2 dr = 1$, with the product of the amplitude C_ℓ and the asymptotically correct Whittaker function W, both taken at large distance r_L,

$$\left(\frac{A}{A-1} C^2 S R_s \right)^{1/2} R(r_L) = C_\ell \frac{W_{-\eta,\ell+1/2}(2kr_L)}{r_L}, \quad (2)$$

where η is the Sommerfeld parameter and k the bound-state wave number. From Eqs. (1), (2), and the definition of R_s, we obtain an expression for the asymptotic normalization coefficient

$$C_\ell^2 = \frac{\sigma_{\text{exp}}}{M(\sigma_{\text{str}} + \sigma_{\text{dif}} + \sigma_{\text{C}})} \left(\frac{r_L R(r_L)}{W_{-\eta,\ell+1/2}(2kr_L)} \right)^2, \quad (3)$$

which is conveniently free of specifications of nuclear-structure parameters. Equation (3) illustrates why the asymptotic normalization coefficient, in the case of the highly peripheral reactions which dominate interactions of very weakly bound systems, can be obtained with better precision [23] than the spectroscopic factor. The essential point is that in such cases the nuclear single-particle cross section samples the extreme nuclear surface.

III. RESULTS AND DISCUSSION

Table II gives an overview of the measured and predicted cross sections. The theoretical cross sections are the product of the single-particle cross section calculated within the eikonal theory of Ref. [8] and the spectroscopic factor from a many-body shell-model calculation. Stripping and diffractive nuclear breakup as well as Coulomb breakup contribute to the total cross section. A center-of-mass correction of magnitude $A/(A-1)$ has to be applied to the spectroscopic factors from the shell model. The quantity R_s given in Table II is defined as the ratio of experimental and theoretical cross section. Assuming the validity of the eikonal reaction theory and of the shell-model description, this number gives the reduction of the single-particle orbital occupancy attributed to short-range correlations.

A. The cross sections for stripping and elastic breakup

As discussed in Sec. II B, it was possible to determine the separate contributions of stripping and elastic breakup. This result, although not very precise, is of some interest since there exists little experimental evidence on the relative role of these two processes. The experiments by Negoita *et al.* [24] found approximately equal contributions of the two mechanisms for ^{8}B on a silicon target. However, with the relatively high Z of the latter, Coulomb breakup, which is well understood, is expected to dominate and the experiment tells us little about the diffractive mechanism. An experiment on the halo nucleus ^{11}Be incident at 41 MeV/nucleon on a ^{9}Be target [25] found the broad angular distribution of the neutrons (out to 20°) expected to be associated with the diffractive process. The corresponding cross section of 120(24) mb is close to half of the inclusive cross section of 290(40) mb, as expected for a pronounced halo state incident on a strongly absorptive target.

The theoretical and experimental results given in Table II provide a more exacting test. For the case of ^{8}B with the results summed over both final states, we obtain for the stripping-to-elastic ratio the values 1.8 (theory) and 2.5(9) (experiment). The corresponding results for ^{9}C are 2.2 (theory) and 2.8(9) (experiment). In both cases the results agree within the experimental errors, but there is still an indication that the diffractive breakup is relatively weaker than predicted. Some uncertainty could come from reactions on the Si nuclei of the detector material, which, as discussed above, have a much stronger contribution from Coulomb breakup, although this part, in principle, is corrected for by the target-out runs. The values of R_s found from the total inclusive cross section and discussed in the following do not depend on the separation of the cross section into diffractive and stripping channels and are more accurate. This is reflected in the errors given.

A more precise check would be possible in a dedicated experiment, preferably on several systems with different l values and separation energies. Such measurements could also be combined with measurements of longitudinal momentum distributions of protons or neutrons and residues, see the theoretical considerations in Ref. [26].
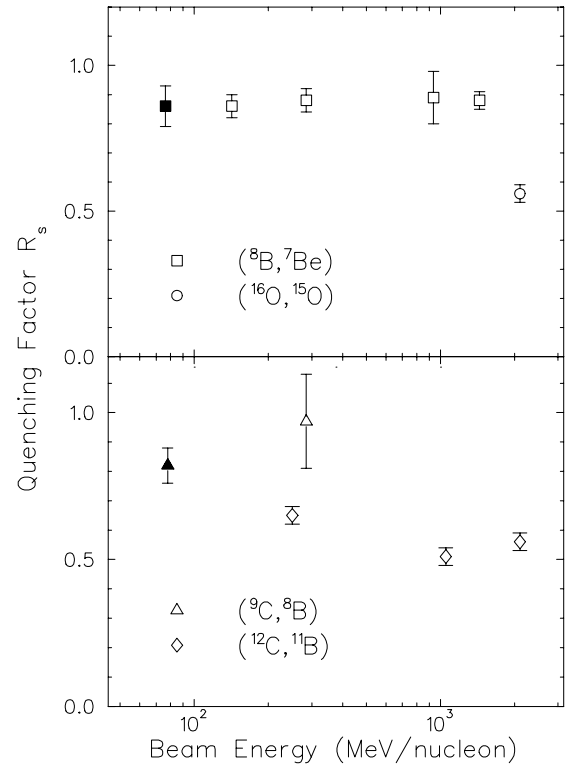

FIG. 4. The apparent reduction in cross section attributed to short-range correlations. The filled (black) symbols are measurements from the present work. The open symbols are from Ref. [12] and the ^{9}C measurement by Blank *et al.* [36] of a one-proton knockout cross section of 48(8) mb at 285 MeV/nucleon.

B. The ^{12}C(^{8}B, ^{7}Be) reaction

Previous work [12] has analyzed this reaction on the basis of data covering the energy range 140 to 1400 MeV/nucleon. The present work adds a data point at 76.4 MeV/nucleon.

The inclusive cross section is found to be 130(11) mb. The main contribution is from the reaction channel leading to the $3/2^-$ ground state. The weaker branch to the $1/2^-$ state at 429 keV has recently been measured separately [27] by observing γ coincidences. As the measured branching ratio of 13(3)% agrees well with 15% calculated from our model [12] for this energy, the short-range reduction factor R_s obtained below is truly characteristic of the ground state.

The parameters and interactions entering the calculation of the theoretical cross sections are the same as those used previously [12]. In particular, the proton-core wave function had radius and diffuseness parameters for the Woods-Saxon potential of $r_0 = 1.254$ and $a = 0.62$ deduced from the experimental Coulomb displacement energy [28]. The results of the theoretical calculation are given in Table II. The ratio R_s between the measured and the expected cross section amounts to 0.86(7) in good agreement with the value of 0.88(4) deduced in Ref. [12] from the four measurements at higher energies. The systematics for R_s is shown in Fig. 4. It was noted by Brown *et al.* that the results for ^{8}B translate into an asymptotic normalization coefficient and via this to an astrophysical factor $S_{17}(0)$ of 21.2(13) eV b. Since the quenching factor R_s from the present experiment is consis-

tent with the one deduced by Brown *et al.* [12], their conclusions remain unchanged. For an overview of the topic, see the literature cited in Refs. [12,31]; in addition, a new direct measurement of the (p,γ) cross section [32] gives 21.2(7) eV b for this quantity.

The proton-removal cross section from ^{8}B was reported by Pecina *et al.* [29] as a by-product in a wider study. Analyzed in the same way as in our work, the result of 80(15) mb at 40 MeV/nucleon on a carbon target translates to $R_s = 0.46(9)$, considerably below our value. In view of the rather large uncertainty of the cross section, which, furthermore, was not the primary objective of this work, it would be premature to conclude that the reaction theory fails at 40 MeV/nucleon.

C. The ^{12}C(^{9}C, ^{8}B) X reaction

Similarly, for the ^{12}C(^{9}C, ^{8}B) X reaction we find a cross section of 54(4) mb. Again, the standard of reference for the absolute occupancies is a truncated shell-model space with effective interactions. For the *p*-shell space, see Brown [30], the PJT interaction gives the spectroscopic factors C^2S to the 2^+ ground state of ^{8}B of 0.93 ($p_{3/2}$) and 0.01 ($p_{1/2}$), or a total *p* spectroscopic factor of 0.94, which we have used in Table II and what follows. Within basically the same model, Millener [33] used an interaction (DJM69) specifically adjusted to the mass $A = 6–9$ region and obtained a value of 0.92. The Cohen-Kurath [34] interaction, referred to as CK616, gave a value of 0.90. Hence, there seems to be a good basis for assuming that the [^{9}C, ^{8}B(2^+)] spectroscopic factor is a good reference value for absolute occupancies.

Still, unexpected changes in the wave function cannot be excluded. It has been suggested [14] that isospin mixing in the proton drip-line nucleus ^{9}C could lead to an excess of $\pi 1s_{1/2}$ in the ground state wave function, a component not included in the model space used here. This might account for the seemingly anomalous isoscalar magnetic moment obtained from the ^{9}C, ^{9}Li mirror pair. The underlying idea is that Coulomb effects could force the appearance of $1s,0d$-shell admixtures at $Z = 6$, where the corresponding effect for neutrons comes into play only at $N = 8$. The effect of such an admixture would be to make the true R_s closer to unity than what we find. Another possible anomaly is that a study [16] of the β decay of ^{9}C found a strong β-strength asymmetry relative to the mirror nucleus ^{9}Li for transitions to the higher states.

The single-particle reaction cross sections were calculated with the same Woods-Saxon parameters as used for ^{8}B. The rms matter radius of the ^{8}B core was taken to be 2.38 fm [35]. The difference in proton separation energies for the initial and final state, 1.296 and 0.1375 MeV, respectively, lead to a mismatch factor $M = 0.976$. Another small correction comes from Coulomb breakup on the carbon target, estimated to have single-particle cross section of 1.1 mb. Combining the reaction calculation with the theoretical spectroscopic factor, we arrive at a calculated cross section of 65.7 mb which can be compared to an experimental value, obtained as described for ^{8}B, of 54(4) mb.

The ratio of the two leads to a quenching factor attributed to short-range correlations of $R_s = 0.82(6)$. Close to the value of 0.88(4) representing (^{8}B,^{7}Be), the result fits in well with a pattern where the reduction factor is 0.5–0.6 for deeply bound proton and neutron states in ^{12}C and ^{16}O and approaches unity for loosely bound halo states [12]. (^{8}B is probably the best case for a proton halo.) It is tempting to speculate that we are dealing with an effect of the nucleon binding energy, and that configuration alone is not decisive for R_s; note that ^{12}C and ^{9}C must have quite similar proton configurations. A previous but less accurate measurement of the inclusive cross section was reported by Blank *et al.* [36], who found a one-proton knockout cross section of 48(8) mb at 285 MeV/nucleon corresponding to $R_s = 0.97(16)$. Both values are shown in Fig. 4.

The full width at half maximum of the energy distribution of the breakup products (stripping and diffraction), could not be determined in the case of the (^{8}B,^{7}Be) reaction due to the residues penetrating partly into the next detector. For ^{9}C, the result was 62(10) MeV. This can be understood by adding in quadrature the contributions from the direct beam (30 MeV), the target thickness (9 MeV), the width of the momentum distribution (40 MeV), the width of the parallel momentum distribution of 130 MeV/c in the lab system (calculated according to Refs. [5,37]), and 32 MeV from the energy loss of the proton in the diffractive channel. The attempt to separate stripping and diffractive breakup to obtain exclusive energy distributions led to no statistically significant results.

D. Astrophysical nucleosynthesis via the ^{8}B(p,γ)^{9}C reaction

This reaction is believed to ignite the explosive hydrogen burning in what is referred to as the hot pp chain [38], and there have recently been several papers attempting to establish the astrophysical rate constant S_{18} or the asymptotic normalization coefficient C_1^2. Our measurement provides the most accurate value of the second quantity. From Eq. (3) together with the data and theoretical parameters given in Table II the result is $C_1^2 = 1.27(10)$ fm^{-1}. The radial wave functions were evaluated at 20 fm, but the exact distance is unimportant.

This is in agreement with other recent work. Beaumel *et al.* [15] measured the reaction $d(^8$B,^{9}C) n at an incident beam energy of 14.4 MeV/nucleon. The experiment was limited by low statistics, giving a relative error of $\pm 25\%$. From eight different combinations of optical potentials they obtained asymptotic normalization coefficients C_1^2 in the range 0.97–1.42 fm^{-1} corresponding to a preferred value of 1.18(34) fm^{-1}. Trache *et al.* [17] analyzed data [36] taken for four different targets (C, Al, Sn, and Pb) at 285 MeV/nucleon, and expressed the outcome in terms of an averaged asymptotic normalization coefficient of 1.22(13) fm^{-1} in excellent agreement with our measurements. Since the heavy targets included in their analysis have substantial contributions from Coulomb breakup, this analysis draws on another reaction mechanism and provides an independent check on

the deduced asymptotic normalization coefficient and spectroscopic factor. Our analysis for the carbon target of Ref. [36] alone, gives 1.50(25) fm^{-1} consistent with all three results.

The papers [15,17] translate their results into astrophysical rate constants S_{18} of 45(13) eV b and 46(6) eV b, respectively. For comparison with this we use a potential-well model in the spirit of Ref. [22]. We take the Woods-Saxon parameters given above, adjust the depth to reproduce the bound-state binding energy, and use the same potential for the continuum s state. This leads to a single-particle S factor at zero energy of 58.6 eV b, which adjusted for the structure parameters of Eq. (2) with numerical values from Table II leads to $S_{18}(0) = 49(4)$ eV b in excellent agreement with the two other values. A new measurement by Hisanaga *et al.* [18] of S_{18} by the method of Coulomb dissociation leads to a somewhat higher result. They cite 77(15) eV b for the energy range 0.2–0.6 MeV, but extrapolated by the slope of their theoretical curve to the lowest energies, the result comes close to 100 eV b, well above the results based on C_1^2. This does not necessarily reflect an experimental problem. We find that the translation from an asymptotic normalization coefficient to the $S_{18}(0)$ can be quite sensitive to the choice of the depth of the potential for the unbound single-particle state.

E. The ^{12}C(^{9}C,^{7}Be) X reaction

It was also possible to extract a value of 98(7) mb for the two-proton removal cross section (^{9}C,^{7}Be). Three main components contribute to the two-proton removal process: (i) one-proton knockout into excited states of ^{8}B and subsequent proton emission from these states, (ii) simultaneous two-proton knockout from a ''double hit'' in the nucleus-nucleus collision, and (iii) protons emitted from the ^{8}B ground state due to shake-off caused by the mismatch of the ^{9}C and ^{8}B wave functions. Component (i) contributes the main fraction to the cross section. From a shell-model calculation, the sum of the spectroscopic factors to states other than the ground state and up to 11 MeV is close to 3, which together with the ground state completes the sum-rule value of 4. From this calculation together with the cross sections from eikonal theory, we estimate the total cross section into unbound states of ^{8}B to be 143 mb. Component (ii) has been estimated within an extension of the eikonal model that neglects the core recoil [39,40] to be $\sigma_{-2p} = 3.45$ mb for a single pair of protons. With four particles in the p shell, combinatorics gives a contribution of 6×3.45 mb$= 21$ mb for the direct two-proton knockout. The shake-off (iii) from the ^{8}B ground state was estimated from the mismatch factor and amounts to 2 mb. The sum of (i), (ii), and (iii) of 166 mb exceeds the experimental value of 98(7) mb. This differs from the case of ^{23}O, recently discussed by Brown *et al.* [40], where a similar estimate for the ^{12}C(^{23}O,^{21}O) X reaction gave $(55+14) = 69$ mb in good agreement with a mea-

sured value of 82(25) mb. The missing cross section in the ^{9}C case almost certainly can be ascribed to other exit channels in the decay of ^{8}B, which open up at low excitation energies such as ^{3}He$+^4$He$+p$ and ^{3}He$+^5$Li.

IV. CONCLUDING REMARKS

There is substantial evidence, see Ref. [11], that the physical occupancies of single-particle states in the shell model may be lower by as much as a factor 0.5–0.6 relative to models based on effective interactions. A recent analysis by Brown *et al.* of single-nucleon knockout reactions at intermediate and high energies suggested that for the case of knockout of a proton from ^{8}B with separation energy S_p of only 0.1375 MeV, the result is much closer to unity. Data presented here for ^{8}B and ^{9}C at close to 80 MeV/nucleon agree with this conclusion. In addition, the five fully consistent ^{8}B results covering the range of beam energies 76–1440 MeV/nucleon, see Fig. 4, give confidence that our eikonal reaction theory is adequate to the task, also in the region of the experimentally very active energy range 50–100 MeV/nucleon. The present paper offers arguments why the theoretical spectroscopic factors for ^{8}B and ^{9}C are known with sufficient precision to serve as theoretical calibration points for the quenching factors summarized in Fig. 4.

For ^{9}C, which is of a certain interest in nuclear astrophysics, the measured cross section translates into the most accurate value, so far, of the asymptotic normalization coefficient $C_1^2 = 1.27(10)$ fm^{-1}. This agrees well with two results reported within the last year. Using a potential model, we translate this into the astrophysical rate coefficient $S_{18}(0) = 49(4)$ eV b. This is lower than the value obtained in a new direct measurement based on Coulomb dissociation. We point out that the translation between asymptotic normalization coefficient and $S(0)$ factor is model dependent.

Finally, our analysis demonstrated a new method for disentangling the contributions from stripping and elastic breakup (nuclear and Coulomb) to the total cross section. Within their experimental uncertainties, the results are consistent with theory and provide the most precise check on the theoretical calculations, so far.

[1] G. R. Satchler, *Direct Nuclear Reactions* (Oxford University Press, New York, 1983).

[2] A. Navin *et al.*, Phys. Rev. Lett. **81**, 5089 (1998).

[3] T. Aumann *et al.*, Phys. Rev. Lett. **84**, 35 (2000).

[4] A. Navin *et al.*, Phys. Rev. Lett. **85**, 266 (2000).

[5] V. Maddalena *et al.*, Phys. Rev. C **63**, 024613 (2001).

[6] J. Enders *et al.*, Phys. Rev. C **65**, 034318 (2002).

[7] P.G. Hansen and B.M. Sherrill, Nucl. Phys. **A693**, 133 (2001).

[8] J.A. Tostevin, J. Phys. G **25**, 735 (1999).

[9] K. Hencken, G. Bertsch, and H. Esbensen, Phys. Rev. C **54**, 3043 (1996).

[10] V.R. Pandharipande, I. Sick, and P.K.A. de Witt-Huberts, Rev. Mod. Phys. **69**, 981 (1997).

[11] G.J. Kramer, H.P. Blok, and L. Lapikas, Nucl. Phys. **A679**, 267 (2001).

[12] B.A. Brown, P.G. Hansen, B.M. Sherrill, and J.A. Tostevin, Phys. Rev. C **65**, 061601(R) (2002).

[13] H. Esbensen and G.F. Bertsch, Phys. Rev. C **64**, 014608 (2001).

[14] M. Huhta *et al.*, Phys. Rev. C **57**, 2790(R) (1998).

[15] D. Beaumel *et al.*, Phys. Lett. B **514**, 226 (2001).

[16] U.C. Bergmann *et al.*, Nucl. Phys. **A692**, 427 (2001).

[17] L. Trache, F. Carstoiu, A.M. Mukhamedzhanov, and R.E. Tribble, Phys. Rev. C **66**, 035801 (2002).

[18] I. Hisanaga *et al.*, Nucl. Phys. (to be published).

[19] D. J. Morrissey, B. M. Sherrill, M. Steiner, A. Stolz, and I. Wiedenhoever, Nucl. Instrum. Methods Phys. Res. B **204**, 90 (2003)

[20] F. Marti, P. Miller, D. Poe, M. Steiner, J. Stetson, and X.Y. Wu, in *Cyclotrons and Their Applications*, edited by F. Marti, AIP Conf. Proc. No. 600 (AIP, Melville, NY, 2001), p. 64.

[21] A.E.L. Dieperink and T. de Forest, Jr., Phys. Rev. C **10**, 533 (1974).

[22] S. Typel and G. Baur, Phys. Rev. C **50**, 2104 (1994).

[23] L. Trache, F. Carstoiu, C.A. Gagliardi, and R.E. Tribble, Phys. Rev. Lett. **87**, 271102 (2001).

[24] F. Negoita *et al.*, Phys. Rev. C **54**, 1787 (1996).

[25] R. Anne *et al.*, Nucl. Phys. **A575**, 125 (1994).

[26] A. Bonaccorso, Phys. Rev. C **60**, 054604 (1999).

[27] D. Cortina-Gil *et al.*, Phys. Lett. B **529**, 36 (2002).

[28] B.A. Brown, A. Csoto, and R. Sherr, Nucl. Phys. **A597**, 66 (1996).

[29] I. Pecina *et al.*, Phys. Rev. C **52**, 191 (1995).

[30] B.A. Brown, Prog. Part. Nucl. Phys. **47**, 517 (2001).

[31] B. Davids, S.M. Austin, D. Bazin, H. Esbensen, B.M. Sherrill, I.J. Thompson, and J.A. Tostevin, Phys. Rev. C **63**, 065806 (2001).

[32] L.T. Baby *et al.*, Phys. Rev. Lett. **90**, 022501 (2003).

[33] D. J. Millener (private communication).

[34] S. Cohen and D. Kurath, Nucl. Phys. **101**, 1 (1967).

[35] A. Ozawa, T. Suzuki, and I. Tanihata, Nucl. Phys. **A693**, 32 (2001).

[36] B. Blank *et al.*, Nucl. Phys. **A624**, 242 (1997).

[37] P.G. Hansen, Phys. Rev. Lett. **77**, 1016 (1996).

[38] M. Wiescher *et al.*, Astrophys. J., Suppl. **343**, 352 (1989).

[39] J. A. Tostevin (unpublished).

[40] B. A. Brown, P. G. Hansen, and J. A. Tostevin, Phys. Rev. Lett. **90**, 159201 (2003).